Evaluation of the Catalytic Capability of cis - and trans -Diquinoxaline Spanned Cavitands

Mami Inoue, Shinsuke Kamiguchi, Katto Ugawa, Shaima Hkiri, Jules Bouffard, David Sémeril, Tetsuo Iwasawa

DOI: 10.1002/ejoc.200((will be filled in by the editorial staff))

Evaluation of Catalytic Capability of *cis*- and *trans*-Diquinoxaline Spanned Cavitands

Mami Inoue,[a] Shinsuke Kamiguchi,[a] Katto Ugawa,[a] Shaima Hkiri,[b,c] Jules Bouffard,[b] David Sémeril*[b] and Tetsuo Iwasawa*[a]

Keywords: Introverted ligand / Cis-spanned cavitands / Diquinoxaline-extended resorcin[4]arene / Gold and Rhodium catalysis

Three new *cis*-diquinoxaline spanned cavitands were synthetized. These *cis*-diphosphinated derivatives were assigned in homogeneous gold-catalyzed dimerization and hydration of alkynes, and rhodium-catalyzed styrene hydroformylation. Results were ranked with those obtained with their *trans*-diphosphinated analogues. The structure-activity relationship realized with these *cis*- or *trans*-flanked cavitands shows that the cis- or trans-positioning of the catalytic center has a direct effect on the effectiveness of the cooperation between the two metallic centers. In fact, the distance between the two metal has a direct effect either on activity or on regioselectivity of a catalytic reaction.

[a] M. Inoue, S. Kamiguchi, K. Ugawa, and Prof. Dr. T, Iwasawa
Department of Materials Chemistry, Ryukoku University
Seta, Otsu, Shiga, 520-2194, Japan
E-mail: iwasawa@rins.ryukoku.ac.jp
p://www.chem.ryukoku.ac.jp/iwasawa/index.html
[b] S. Hkiri, J. Bouffard, and Dr. D. Sémeril
Synthèse Organométallique et Catalyse, UMR-CNRS 7177,
Université de Strasbourg, 4 rue Blaise Pascal, 67070 Strasbourg Cedex, France
E-mail: dsemeril@unistra.fr
[c] S. Hkiri
Faculté des Sciences de Bizerte, Université de Carthage
7021 Jarzouna, Bizerte, Tunisia

Introduction

Resorcin[4]arene-cavitand, able to carry out a catalytic reaction, is an emerging supramolecule that mimics enzymatic catalysis and achieves marvelous chemical transformations from the viewpoint of green chemistry.[1] The cavitands have strong resemblances in two points to natural enzymes: one, cavitands are partly open, guest substrates readily fill the space, enter and leave; the second, cavitands are endowed with gently curved concave large enough to accommodate catalytic centers. Despite the relevant role played by catalytic cavitands, such a class of cavitands is underrepresented owing to synthetic difficulties.[3,4] To make supramolecular cavitands those weigh over MW *ca*. 1000 preparatively in pure form is a basically embarrassing synthesis. When we attempt to introduce reactive centers inside the hydrophobic pockets, isomeric production of in- and outwardly oriented cavitands towards the pockets often occurs. Hence, we chemists are now always struggling to understand even basic aspect of cavitand catalysis. It might be quite a challenge for us to imitate enzymatic virtue that Mother Nature has meticulously created for more than long, long four billion years, because synthetic chemistry has been in just one or two hundred-year-period history since Friedrich Wöhler synthesized urea from ammonium cyanate.[5,6]

Recently, we have developed for catalytic applications *trans*-di-quinoxaline-spanned resorcin[4]arenes.[7] An introverted bis-gold cavitand was found to be efficient in the dimerization of two different terminal alkynes.[8] A second type of gold cavitand, in which a lewis acid gold cation was associated to a lewis basic P=O moiety, displayed high regioselectivities in addition of H_2O to unsymmetrical triple bonds; for example, 3-octanone was obtained in 91 % yield starting from 3-octyne.[9] Although the advantage of cavitand catalysis in selective transformations are obvious, but systematic studies of structure-activity relationship remains rare. Particularly, from the viewpoint of basic research, comprehension of mechanistic aspects awaits upgrading, enhancement, and accomplishment. Herein we report a structure-activity relationship of phosphinated cavitands in transition metal-

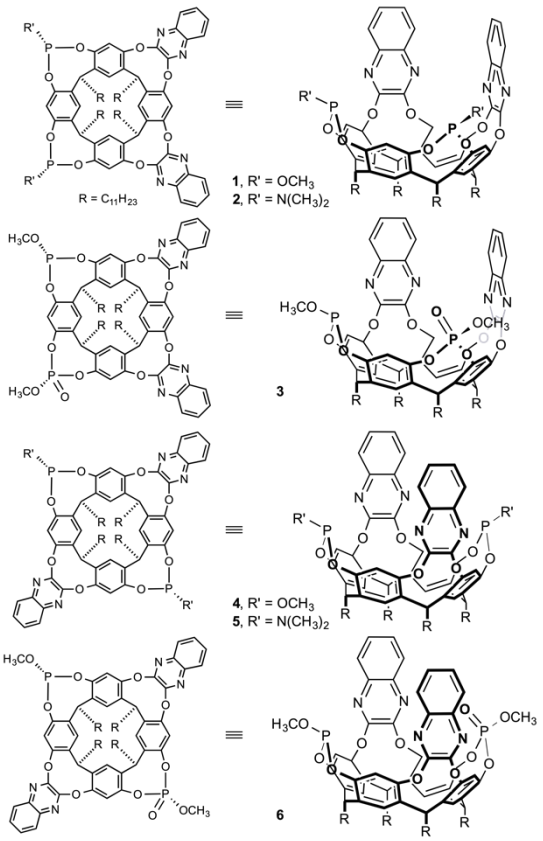

Figure 1. *Cis*-**1**-**3** and *trans*-**4**-**6** di-quinoxaline-spanned resorcin[4]arenes.

catalyzed reactions. We prepared new *cis*-type P(III) (**1** and **2**) and mixed P(III)/P(V) (**3**) extended cavitands, which are structurally similar to previously reported *trans*-type **4**, **5**, and **6** derivatives (Figure 1): those are used as ligands in gold- and rhodium-catalysis. The question we pursue here is *"How does the difference between these trans- and cis-arrangements affect the catalytic activity and selectivity?"*

Results and Discussion

The synthesis of *cis*-**1** starts with a reaction between resorcin[4]arene and 2,3-dichloroquinoxaline (Scheme 1(a)). Preparation of *cis*-positioned di-quinoxaline-spanned resorcin[4]arene was laborious[10] and required the use of DABCO (1,4-diazabicyclo[2.2.2]octane) and pyridine improved the chemical yield to 22%. The obtained *cis*-positioned tetra-ol cavitand reacted, in the presence of a base in refluxing toluene, with $P(OCH_3)_3$ to give two of the three possible isomers ("out-out", "in-out", and "in-in"). The two compounds were carefully separated by silica-gel column chromatography and were isolated in 44% and 22% yield for the be "out-out" **1** and "in-out" *iso*-**1**, respectively (Scheme 1(b)).[11] Orientation of the lone pair of the phosphorus atoms were deduced from their ^{1}H NMR spectra. In the case of **1**, its ^{1}H NMR spectrum reveals one doublet located at 3.87 ppm ($^3J_{PH}$ = 8.6 Hz) for the two "out-out" POCH_3; in the spectrum of *iso*-**1**, two doublets at 3.87 ppm ($^3J_{PH}$ = 8.6 Hz) and at 3.20 ppm ($^3J_{PH}$ = 12.6 Hz), which can be attributed to the two "in-out" POCH_3 protons (Figure 2 (a) and (b)). The latter up field-shifted doublet (δ = 3.20 ppm) results from anisotropic effects of the aromatic π clouds and the OCH_3 group inwardly oriented. Consequently, in cavitand **1**, the two $POCH_3$ moieties are outwardly oriented as confirmed by the chemical shifts of the outwardly oriented POCH_3 groups in the well know cavitands **4** (δ = 3.97 ppm, $^3J_{PH}$ = 8.7 Hz) and *iso*-**4** (Figure 3 (a); δ = 3.98 ppm, $^3J_{PH}$ = 8.3 Hz and δ = 3.10 ppm, $^3J_{PH}$ = 12.4 Hz) (Figure 2 (c) and (d)). Interestingly, oxidation of only one phosphorus atom of *iso*-**1** could be carried out in the presence of mCPBA (*meta*-chloroperbenzoic acid), cavitand **3** was isolated in 30% yield (Scheme 1(c)).[12]

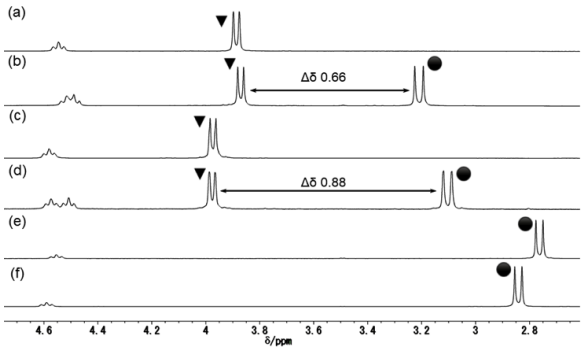

Figure 2. Portions of ^{1}H NMR spectra (400 MHz, $CDCl_3$) of (a) **1**, (b) *iso*-**1**, (c) **4**, (d) *iso*-**4**, (e) **2**, and (f) **5**. The peaks labeled with black colored-circle and black colored-triangle correspond to inward- and outward-oriented POCH_3 or PN(CH_3)$_2$ groups, respectively.

Di-phosphoramidite derivative *cis*-**2** was obtained by reaction between the tetra-ol resorcinarene and $P[N(CH_3)_2]_3$ in the presence of NEt_3 at 75°C in toluene. Although, after 1 hour, TLC displayed mostly a single spot, due to decomposition degradation during silica-gel column chromatography, compound *cis*-**2** was isolated in only 44% yield (Scheme 1(a)). Its ^{1}H NMR spectrum exhibits one doublet located at 2.76 ppm ($^3J_{PH}$ = 10.5 Hz), which could be attributed to the two outwardly directed PN(CH_3)$_2$ moieties. A similar signal at 2.85 ppm ($^3J_{PH}$ = 11.05 Hz) was previously observed in the cavitand *trans*-**5** (Figure 2 (e) and (f)).[13]

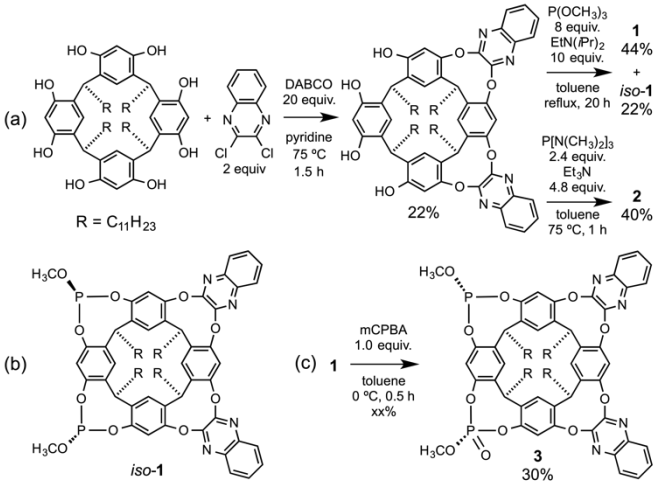

Scheme 1. (a) Synthesis of *cis*-**1** and *cis*-**2**; (b) *iso*-**1** bearing both inward- and outward $POCH_3$ groups; (c) synthesis of *cis*-**3** (mCPBA = *meta*-chloroperbenzoic acid).

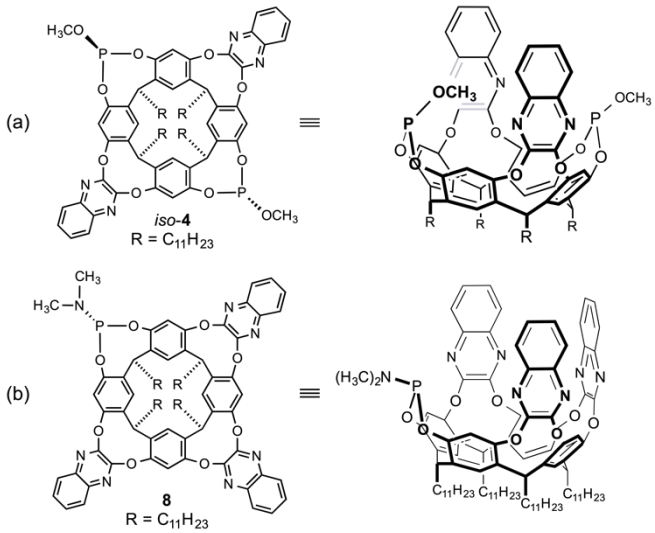

Figure 3. Structures of (a) *iso*-**4** that has one inward P-OMe and one outward P-OMe, and (b) mono-phosphoramidite **8** that was flanked by three quinoxaline moieties.

The conformational flexibility of tetra-quinoxaline-spanned resorcin[4]arenes is well known and can fluctuate between vase (close) and kite (open) conformations. The conformation of the macrocycle could be deduced from its ^{1}H NMR spectrum and more particularly from the chemical shift of methine protons directly beneath quinoxaline moieties. A chemical shift around 5.5 ppm indicates a vase conformer, whereas a chemical shift around 3.7 ppm reveals a kite form.[14] For our four new compounds (**1**, *iso*-**1**, **2** and **3**), ^{1}H NMR investigations carried out in $CDCl_3$ and [D_8]toluene, clearly indicate a vase conformation of the cavitands, the methine protons appear at 5.73 (**1**), 5.76 and 5.71 (*iso*-**1**), 5.70 (**2**), 5.79-5.71 (**3**) ppm in $CDCl_3$ and at 6.14 (**1**), 6.15 and 6.08 (*iso*-**1**), 6.15 (**2**) and 6.20 and 6.11 (**3**) ppm in [D_8]toluene. Then,

we interested in the difference in π-clouded environment between *cis*- and *trans*-walled cavitands. For that, we compared the chemical shifts of the CH_3 proton of the $POCH_3$ moieties in cavitands *iso*-**1** and *iso*-**4**. As shown in Figure 2 (b) and (d), the Δδ (differences in the chemical shifts between inward- and outward-oriented $POCH_3$) are 0.66, and 0.88 for *iso*-**1** and *iso*-**4**, respectively. These results are important evidences suggesting that the *trans*-walls create a definite compartment that is more heavily influenced by the π-clouds than the compartment of the *cis*-walled cavitand.

Phosphites **1** and **3** readily formed complexes with AuCl•$S(CH_3)_2$. Using a Au/P ratio of 1:1.2 in toluene, after 0.5 h *cis*-**1**•$(AuCl)_2$ and *cis*-**3**•AuCl complexes were isolated in 100% and 63% yield, respectively (Scheme 2). The latter gold complexes were tested in cross- and homo-dimerization of alkynes as well as in hydration of di-substituted alkynes. Their performances in catalysis will be ranking with the previous reported *trans*-**4**•$(AuCl)_2$ and *trans*-**6**•AuCl complexes.[7b,15]

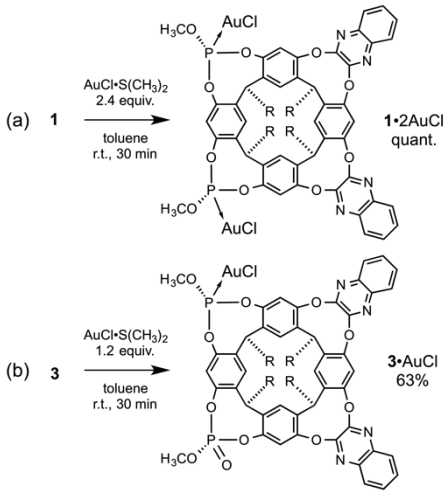

Scheme 2. Synthesis of (a) **1**•$(AuCl)_2$ and (b) **3**•AuCl complexes.

For the gold-catalyzed terminal alkynes dimerization, the runs were carried out using 1 mol % of *cis*-**1**•$(AuCl)_2$ or *trans*-**4**•$(AuCl)_2$ complex and 2 mol % of AgOTf in toluene at room temperature for 20 h (Scheme 3). Using precatalyst *cis*-**1**•$(AuCl)_2$, whether for cross-dimerization of ethynylbenzene and 1-octyne or for homo-dimerization of 1-octyne, only 2-octanone (**7c**), coming from hydration of octyne, was observed in 29% and 35% yield, respectively. These results contrast with those observed when the tests were repeated using the *trans*-diquinoxaline spanned *trans*-**4**•$(AuCl)_2$ complex. The letter led only to the formation of dimeric products, with a ratio hetero-/homo-dimer of **7a**/**7b** = 75:25 when a mixture of ethynylbenzene and 1-octyne was employed or quantitatively to the dimer **7b** in the case of dimerization of 1-octyne. These results clearly show the importance of the positioning of the two gold center on the resorcin[4]arene skeleton. Using bis-gold complexes with *cis*- and *trans*-walled cavitands led to different type of active species and catalytic outcome.

Differences in activity and regioselectivity could also be highlighted in the gold-catalyzed hydration of internal alkynes using mixed P(III)/P(V) extended cavitands, in which the two phosphorus atoms are *cis*- or *trans*-positioning, *cis*-**3**•AuCl or *trans*-**6**•AuCl complexes, respectively. For hydration of ethynylbenzene, the *cis*-**3**•AuCl complex led to low activity and selectivity, the products, 1-phenyl-1-butanone (**7d**) and 1-phenyl-2-butanone (**7e**) were obtained in 5% and 10% yield, respectively. While repeating the run with precatalyst *trans*-**6**•AuCl, the compounds **7d** and **7e** were isolated in 2% and 88% yield, respectively. A better regioselectivity was also observed when *trans*-**6**•AuCl complex was employed in the hydration of 3-octyne, the ratio 4-octanone (**7f**)/3-octanone (**7g**) = 9:91. The ratio **7f**/**7g** decrease to 46:54 when complex *cis*-**3**•AuCl was used (Scheme 4).

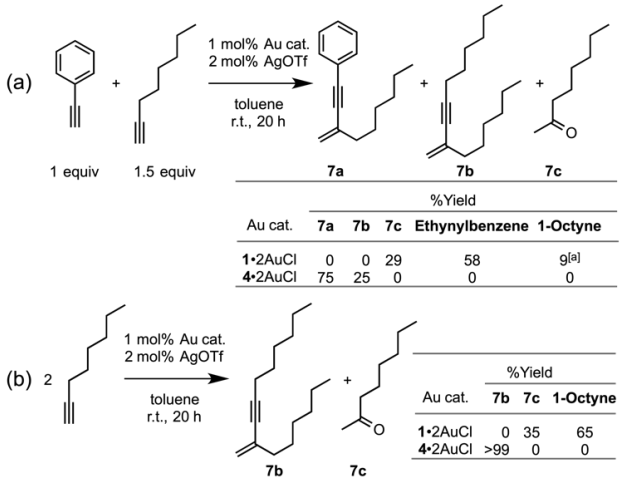

Au cat.	7a	7b	7c	%Yield Ethynylbenzene	%Yield 1-Octyne
1•2AuCl	0	0	29	58	9[a]
4•2AuCl	75	25	0	0	0

Au cat.	7b	7c	%Yield 1-Octyne
1•2AuCl	0	35	65
4•2AuCl	>99	0	0

Scheme 3. Catalytic evaluation of *cis*-**1**•$(AuCl)_2$ and *trans*-**4**•$(AuCl)_2$ in (a) cross-dimerization and (b) homo-dimerization (see Experimental Section).

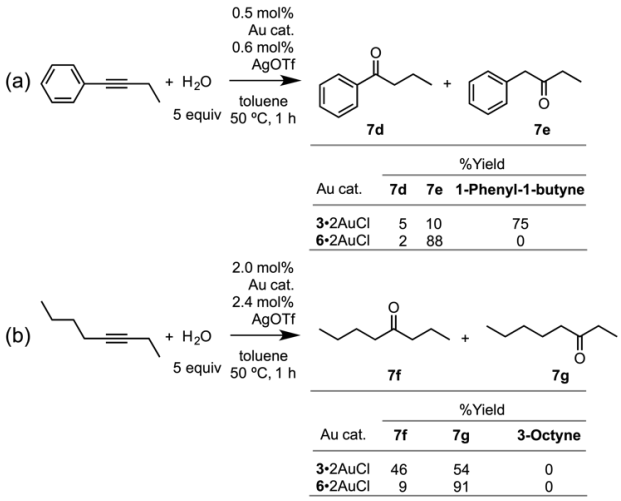

Au cat.	7d	7e	%Yield 1-Phenyl-1-butyne
3•2AuCl	5	10	75
6•2AuCl	2	88	0

Au cat.	7f	7g	%Yield 3-Octyne
3•2AuCl	46	54	0
6•2AuCl	9	91	0

Scheme 4. Catalytic evaluation of *cis*-**3**•AuCl and *trans*-**6**•AuCl in hydration reactions of (a) ethynylbenzene, and (b) 3-octyne (see Experimental Section).

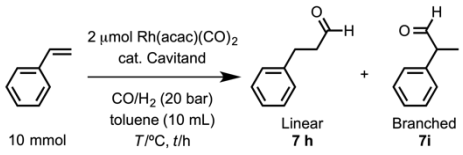

Scheme 5. Rhodium-catalyzed styrene hydroformylation

The three cavitands bearing phosphoramidite moieties (*cis*-**2**, *trans*-**5** and **8**[16]) were assessed in styrene hydroformylation

(Scheme 5). The catalytic systems were generated *in situ* by mixing ligand with Rh(acac)$(CO)_2$ precursor and the reactions were carried out in toluene under 20 bar of CO/H_2 (1:1) with a styrene/Rh ratio of 5000.

In a first series of tests, conduced at 80°C during 24h, the cavitand/Rh ratio (P/Rh) was studied (Table 1). Variation of the number of phosphorous atoms per rhodium atom ratio to 2 to 10, as general trends, we observed a decrease of the conversion when the amount of ligand increased. For example, using mono-phosphoramidite **8**, conversions of 64% and 54% were measured when P/Rh ratios of 2 and 10 were employed, respectively (Table 1, entries 7 and 9). Di-phosphoramidites *cis*-**2** and *trans*-**8** were more efficient than mono-phosphoramidite **8**, conversions of 96%, 99% and 64%, respectively, were observed with a P/Rh ratio of 4 (Table 1, entries 2, 5 and 8). Interestingly, the regioselectivity of the reaction was not affected by the presence of excess of ligand for *cis*-**2** (l/b = 35/65) contrary to the other two (Table 1, entries 1-3). It is noteworthy, in the case of ligand *trans*-**5**, that the P/Rh ratio drastically affects the regioselectivity of the reaction. The proportion of branched aldehyde increase with the number of extra-added ligand, 2-phenylpropanal was formed in 48% and 78% selectivity with P/Rh ratio of 2 and 10, respectively (Table 1, entries 4 and 10). Note that the regioselectivities were similar when either *trans*-**5** or **8** when were employed in large excess, branched aldehydes were formed in 78% and 76%, respectively (Table 1, entries 6 and 9).

Table 1. Evaluation of phosphoramidites *cis*-**2**, *trans*-**5**, and **8** in styrene hydroformylation: influence of the P/Rh ratio.[a]

Entry	P/Rh[b]	Ligand	Conv./%	Product Distribution	
				Linear/%	Branched/%
1	2		91	35	65
2	4	*cis*-**2**	96	34	66
3	10		100	37	63
4	2		98	52	48
5	4	*trans*-**5**	99	39	61
6	10		99	22	78
7	2		64	31	69
8	4	**8**	64	31	69
9	10		54	24	76

[a] Reactions were carried out in conditions of Scheme 5 at 80 ºC for 24 h. The conversions and products distributions were determined by GC (*n*-decane as internal standard) and by ^{1}H NMR. [b] Ratio of phosphorous atoms per rhodium atom.

In a second series of runs, we investigated the influence of the temperature from 60°C to 140°C after 5 h reaction time with a P/Rh ratio of 2 (Table 2). As general trends, the conversion increase with the temperature, around 120°C, and the regioselectivity of the catalysis change from mainly branched aldehyde at low temperature to mainly linear aldehyde at high temperature. For example, using *trans*-**5** ligand, conversion of 52% with a l/b ratio of 16/84 were observed at 60°C against a full conversion with a l/b ratio of 64/36 at 120°C (Table 1, entries 8 and 13). For the tests carried out at 140°C, lower conversions came from decomposition of the catalyst at high temperature (Table1, entries 7, 14 and 21). We can observe that di-phosphoramidite (*cis*-**2** and *trans*-**5**) led to higher activities than mono-phosphoramidite **8**, especially at low temperature. In fact, at 60°C, conversions of 59%, 52% and 11% were measured when ligand *cis*-**2**, *trans*-**5** and **8**, were employed, respectively (Table 2, entries 1, 8 and 15). Similarly, a higher regioselectivity toward linear aldehyde was measured when *cis*-**2** and *trans*-**5** were used rather than **8**, proportion of 35 %, 51% and 31% of 3-phenylpropanal were obtained, respectively (Table 2, entries 2, 9 and 16). Note that during runs, once formed, the *in situ* generated catalysts were stables as observed by similar catalytic outcome analyzed during the first 5 h of hydroformylation reactions carried out at 120°C (Table 1, entries 4-6, 11-13 and 18-20). We can also observed that, at 60°C, *cis*-**2** led to a faster catalytic system with a higher proportion of linear aldehyde than its homologue di-phosphoramidite *trans*-**5**, conversion of 59% (linear aldehyde 33%) against 52% (16% of linear aldehyde), respectively (Table 2, entries 1 and 8). The main differences observed between the two di-phosphoramidites, is that *cis*-**2** led to less thermically stable active species than those formed with *trans*-**5**. In fact, at temperature of 120°C or higher, lower activities were measured when *cis*-**2** was employed rather than *trans*-**5** (Table 2, entries 5-7 and 12-14) and at the end of the runs carried out with *cis*-**2**, carful observation of the reaction mixture shown the formation of traces of black insoluble materials, probably rhodium colloids.

Table 2. Evaluation of phosphoramidites *cis*-**2**, *trans*-**5**, and **8** in styrene hydroformylation: influence of the temperature.[a]

Entry	Cavitand	*T*/ºC	*t*/h	Conv./%	Product Distribution	
					Linear/%	Branched/%
1		60	5	59	33	66
2		80	5	88	35	65
3		100	5	92	56	43
4	*cis*-**2**	120	0.5	41	66	34
5		120	2	48	63	37
6		120	5	69	65	35
7		140	5	60	62	38
8		60	5	52	16	84
9		80	5	75	51	49
10		100	5	89	58	42
11	*trans*-**5**	120	0.5	48	56	44
12		120	2	89	63	37
13		120	5	100	64	36
14		140	5	100	64	36
15		60	5	11	18	82
16		80	5	40	31	68
17		100	5	82	58	42
18	**8**	120	0.5	17	56	44
19		120	2	69	66	34
20		120	5	91	64	36
21		140	5	54	68	32

[a] Reactions were carried out in conditions of Scheme 5 with P/Rh = 2 (ratio of phosphorous atoms per rhodium atom). The conversions and products distributions were determined by GC (*n*-decane as internal standard) and by ^{1}H NMR.

From these experiments, several information about the nature of the catalytic systems generated from the three ligands could be deduced:

- In the case of mono-phosphoramidite **8**, due to the steric hindrance generated by the three quinoxaline moieties, formation of RhL_2 complex should be exclude. Generation of singly ligated active species favor the formation of Rh(η^3-styrenyl)(**8**)$(CO)_2$ intermediate over the less stable Rh(σ-ethylphenyl)(**8**)$(CO)_2$ species and *in fine*, favor the formation of the branched aldehyde,[17] at less at low temperature. At high temperature, thermal agitation generates strong steric interactions between the coordinated substrate and the cavity

wall; such metal confinement favors the formation of the linear aldehyde.[18]

- For the di-phosphoramidite *trans*-**5**, due to the distance between the two phosphorus atoms (9.7 Å measured on the RX structure of *trans*-**5**•$(AuCl)_2$ complex[8]), formation of rhodium-chelate complexes should be exclude. Nevertheless, the proximity of two coordinated rhodium atoms, on the same cavitand, may allow to consider a cooperation between these two metal centers.[19] In fact, the higher activity and the selectivity toward the linear aldehyde regarding ligand **8** are arguments in that sense. Furthermore, when a large excess of *trans*-**5** was employed, in that case, we can assume that only one atom of rhodium is coordinated to the ligand, the second phosphorus atom remained free, regioselectivity of the reactions was similar to that obtained when mono-phosphoramidite **8** was employed (*vide supra*).
- With di-phosphoramidite *cis*-**2**, according to molecular modeling, the distance between the two phosphorus atoms (around 6.5 Å) was to important to allow the formation of rhodium-chelate complexes. The shorter distance, compare to the *trans*-**8** isomer, should reinforce the cooperation between the two metallic centers, which led to a more efficient catalytic system as observed at low temperature. However, the shorter distance may be responsible of the low thermal stability of the corresponding binuclear complexes and the formation of rhodium colloids. The *cis*-positioning of the phosphorus atoms led also to a more open cavitand compare to *trans*-**8**, the steric pressure excess by the two quinoxaline walls was reduced and consequently, the proportion of branched aldehyde formed was more important than when isomer *trans*-**8** was employed.

Conclusions

In summary, three cavitands having a *cis*-arrangement of two quinoxaline walls (*cis*-**1**, *cis*-**2**, and *cis*-**3**) were successfully synthesized. These cavitands, in which two catalytic centers are inwardly oriented, provide new architecture for transition metal catalysis. Gold-catalyzed dimerization and hydration of alkynes and rhodium-catalyzed styrene hydroformylation were carried out with these cis-type cavitands. Comparative studies with analogues trisquinoxaline and *trans*-diquinoxaline spanned cavitands allow us to evaluate the structure-activity relationship between *cis*- and *trans*-walls flanked-cavitands. The catalytic results strongly suggest three salient features. Firstly, *cis*-positioning phosphorus atoms led to a more open cavitands, which leads to a highly reactive species toward solvent impurities, for example in the dimerization of alkynes, traces of water present in toluene. Secondly, the less impeded environment around the metal center reduced or modified the regioselectivities of the reactions compare to those observed with *trans*-spanned ligand. Thirdly, the distance between the two phosphorus atoms is shorter in the case of *cis*- than *trans*-cavitands. Although a shorter distance promotes cooperation between the two metal centers, as observed in the styrene hydroformylation, it favors the degradation of the active species and the formation of rhodium colloids. To the best of our knowledge, this work represents the first examples in homogeneous catalysis of comparative studies involving ligands built on extended cavitands having a *cis*- or a *trans*-positioning of two active centers. Further developments of hybrid catalysts grafted on extended cavitands are ongoing and will be reported in due course.

Experimental Section

General Methods: All reactions sensitive to air or moisture were carried out in anhydrous conditions under argon or nitrogen atmosphere. Dry solvents were purchased and used without further purifications. All reagents were purchased and used without further purifications. Analytical thin layer chromatography was carried out on Merck silica $60F_{254}$. Column chromatography was carried out with silica gel 60 $_N$ (Kanto Chemical Co.). LRMS and HRMS were reported on the basis of TOF (time of flight)-MS (MADI-TOF or LCMS-IT-TOF), and DART (Direct Analysis in Real Time)-MS. ^{1}H, ^{13}C{^{1}H} and ^{31}P{^{1}H} NMR spectra were recorded with a 5 mm QNP probe at 400 MHz and 100 MHz, respectively. Chemical shifts are reported in δ (ppm) with reference to residual solvent signals [^{1}H NMR: $CHCl_3$ (7.26), toluene (2.08); ^{13}C NMR: $CDCl_3$ (77.0); ^{31}P shifts are given with respect to external H_3PO_4]. Signal patterns are indicated as s, singlet; d, doublet; t, triplet; q, quartet; m, multiplet; br, broad. Assignment of ^{13}C NMR was carefully performed with labeling the corresponding numbers those were listed in ^{13}C NMR spectra.

Synthesis of 1 and *iso*-1: (see Scheme 1 (a) and (b)) To the Schlenk tube charged with a solution of the tetra-hydroxy *cis*-cavitand (407 mg, 0.3 mmol) in dry toluene (3 mL) under N_2 at 135ºC, $EtN(iPr)_2$ (0.52 mL, 3.0 mmol) and $P(OCH_3)_3$ (0.29 mL, 2.4 mmol) were added. After stirred for 6 h, the reaction mixture was cooled to room temperature and concentrated to give 457 mg of crude products as pale yellow solid materials. Purification by silica-gel column chromatography (eluent: hexane/EtOAc, 19/1) afforded 195 mg of **1** ("out-out") as white solid materials in 44% yield and 98 mg of *iso*-**1** ("in-out") as white solid materials in 22% yield.

Data for **1**: ^{1}H NMR (400 MHz, $CDCl_3$) 8.41 (s, 1H), 7.98 (d, J = 8.2 Hz, 2H), 7.82 (d, J = 8.2 Hz, 2H), 7.62-7.52 (m, 4H), 7.38 (s, 2H), 7.21 (s, 3H), 7.17 (s, 1H), 6.46 (s, 1H), 5.73 (t, J = 7.8 Hz, 2H), 4.54 (t, J = 7.8 Hz, 2H), 3.88 (d, $^3J_{PH}$ = 8.6 Hz, 6H, POCH_3), 2.30-2.17 (m, 8H), 1.43-1.27 (m, 72H), 0.90-0.87 (m, 12H) ppm; ^{1}H NMR (400 MHz, [D_8]toluene) 8.82 (s, d1H), 7.85 (d, J = 8.2 Hz, 2H), 7.78 (s, 2H), 7.69 (s, 2H), 7.66 (s, 2H), 7.58 (s, 1H), 7.49 (d, J = 8.2 Hz, 2H), 7.18 (dd, J = 8.1, 7.4 Hz, 2H), 7.06-7.01 (m, 2H), 6.32 (s, 1H), 6.14 (t, J = 8.1 Hz, 2H), 4.87 (t, J = 7.8 Hz, 2H), 3.65 (d, $^3J_{PH}$ = 8.6 Hz, 6H, POCH_3), 2.46-2.35 (m, 8H), 1.50-1.29 (m, 72H), 0.97-0.92 (m, 12H) ppm; ^{13}C{^{1}H} NMR (100 MHz, $CDCl_3$) 153.2 (C^{15}), 153.03 (C^{10}), 152.98 (C^7), 152.9 (C^8), 147.3 (C^{17}), 147.2 (C^{21}), 147.10 (C^5), 147.06 (C^6), 140.03 (C^{13}), 137.6 (d, $J_{C,P}$ = 2.6 Hz, C^{19}), 136.5 (C^{12}), 135.3 (C^{20}), 129.6 (C^1), 129.4 (C^4), 128.4 (C^2), 128.2 (C^3), 123.8 (C^{18}), 122.9 (C^{14}), 122.3 (C^{13}), 119.2 (C^{22}), 118.1 (C^{16}), 117.4 (C^9), 50.4 (d, $J_{C,P}$ = 2.6 Hz, C^{23}), 35.9, 34.4, 32.9, 32.3 (many peaks are overlapped), 30.1 (many peaks are overlapped), 29.8 (many peaks are overlapped), 28.4, 28.3, 23.1 (many peaks are overlapped), 14.5 (many peaks are overlapped) ppm; ^{31}P{^{1}H} NMR (162 MHz, $CDCl_3$) 127.3 ppm; MS (ESI) *m/z*: 1512 [M + Cl]$^-$; IR (neat): 2922, 2851, 1606, 1578, 1482, 1412, 1332, 1158, 1029, 759 cm^{-1}; HRMS (ESI) calcd for $C_{90}H_{118}N_4O_{10}P_2Cl$: 1511.8017 [M + Cl]$^-$, Found: 1511.8000.

Data for *iso*-**1**: ^{1}H NMR (400 MHz, $CDCl_3$) 8.36 (s, 1H), 7.99 (d, J = 8.0 Hz, 1H), 7.97 (d, J = 7.8 Hz, 1H), 7.84 (d, J = 8.1 Hz, 1H), 7.64 (d, J = 8.2 Hz, 1H), 7.64-7.51 (m, 4H), 7.39 (s, 1H), 7.28 (s, 1H), 7.22 (s, 2H), 7.15 (s, 1H), 7.11 (s, 1H), 6.31 (s, 1H), 5.76 (t, J = 7.8 Hz, 1H), 5.71 (t, J = 7.8 Hz, 1H), 4.53-4.46 (m, 2H), 3.87 (d, $^3J_{PH}$ = 8.6 Hz, 3H, POCH_3), 3.21 (d, $^3J_{PH}$ = 12.6 Hz, 3H, POCH_3), 2.29-2.17 (m, 8H), 1.41-1.27 (m, 72H), 0.90-0.87 (m, 12H) ppm; ^{1}H NMR (400 MHz, [D_8]toluene) 8.82 (s, 1H), 8.03 (d, J = 8.3 Hz, 1H), 7.81 (d, J = 8.3 Hz, 1H), 7.69 (s, 1H), 7.66 (s, 1H), 7.63 (s, 1H), 7.56 (s, 2H), 7.50 (s, 1H), 7.42 (d, J = 8.2 Hz, 1H), 7.39 (d, J = 8.2 Hz, 1H), 7.26 (dd, J = 8.2, 7.3 Hz, 1H), 7.18 (dd, J = 8.2, 7.3 Hz, 1H), 7.05-7.01 (m, 2H), 6.38 (s, 1H), 6.15 (t, J = 8.1 Hz, 1H), 6.08 (t, J = 8.1 Hz, 1H), 4.91 (t, J = 7.9 Hz, 1H), 4.75 (t, J = 7.9 Hz, 1H), 3.72 (d, $^3J_{PH}$ = 8.6 Hz, 3H, POCH_3), 2.43-2.32 (m, 8H), 2.04 (d, $^3J_{PH}$ = 12.4 Hz, 3H, POCH_3), 1.48-1.29 (m, 72H), 0.95-0.93 (m, 12H) ppm; ^{13}C{^{1}H} NMR (100 MHz, $CDCl_3$) 153.3 (C^{40}), 153.23 (C^8), 153.19 (C^{32}), 153.1 (C^{19}), 153.0 (C^{16}), 152.9 (C^7), 152.7 (C^{15}), 152.4 (d, $J_{C,P}$ = 1.2 Hz, C^{38}), 148.8 (C^{24}), 148.6 (d, $J_{C,P}$ = 6.2 Hz

C^{30}), 148.5 (C^{26}), 147.3 (d, $J_{C,P}$ = 4.5 Hz, C^{17}), 146.6 (d, $J_{C,P}$ = 2.4 Hz, C^{37}), 140.34 (C^{13}), 140.31 (C^{6}), 140.28 (C^{14}), 140.2 (C^{5}), 137.8 (d, $J_{C,P}$ = 2.6 Hz, C^{36}), 136.54 (C^{21}), 136.45 (C^{34}), 135.9 (C^{23}), 135.7 (C^{27}), 135.4 (C^{28}), 134.8 (C^{35}), 134.4 (C^{29}), 129.8 (C^{2}), 129.7 (C^{11}), 129.5 (C^{3}), 129.4 (C^{10}), 128.5 (C^{22}), 128.3 (C^{33}), 127.8 (C^{20}), 124.1 (C^{12}), 123.1 (C^{1}), 122.6 (C^{9}), 121.7 (C^{4}), 119.1 (C^{25}), 118.0 (C^{39}), 117.7 (C^{31}), 116.8 (C^{18}), 51.9 (d, $J_{C,P}$ = 22.2 Hz, C^{41}), 50.2 (d, $J_{C,P}$ = 2.6 Hz, C^{42}), 36.7, 35.9, 34.5, 34.4, 32.8, 32.5, 32.3 (many peaks are overlapped), 31.8, 31.1, 30.2, 30.12, 30.09 (many peaks are overlapped), 30.05, 30.01, 29.78, 29.75, 28.4, 28.3, 23.1, 23.0 (many peaks are overlapped), 14.5 (many peaks are overlapped) ppm; $^{31}P\{^{1}H\}$ NMR (162 MHz, $CDCl_3$) 125.6, 110.6 ppm; MS (ESI) *m/z*: 1512 [M + Cl]$^-$; IR (neat): 2922, 2851, 1578, 1482, 1412, 1352, 1146, 1029, 760 cm^{-1}; HRMS (ESI) calcd for $C_{90}H_{118}N_4O_{10}P_2Cl$: 1511.8021 [M + Cl]$^-$, Found: 1511.8021.

Synthesis of 2: (see Scheme 1 (a)) To the tetra-hydroxy *cis*-cavitand platform (272 mg, 0.2 mmol) in a 20 mL Schlenk tube under Ar were added toluene (2 mL) and Et_3N (0.13 mL, 0.96 mmol). After the mixture was stirred for 10 min, $P[N(CH_3)_2]_3$ was added and the reaction mixture was heated at 75°C for 1 h. The mixture was allowed to cool to room temperature, filtered, washed with toluene, and then the filtrate was concentrated in vacuum to give 309 mg of crude products. Purification by short-plugged column chromatography (eluent, $CHCl_3$ only) afforded 138 mg of white solid materials, which were recrystallized from EtOH/EtOAc (8 mL/4.5 mL) to yield **2** in 40% (120 mg) as colorless crystals. ^{1}H NMR (400 MHz, $CDCl_3$) 8.39 (s, 1H), 7.99 (dd, *J* = 8.5, 8.4 Hz, 2H), 7.80 (dd, *J* = 8.2, 1.4 Hz, 2H), 7.61-7.51 (m, 4H), 7.32 (s, 2H), 7.19 (s, 1H), 7.18 (s, 2H), 7.12 (s, 1H), 6.33 (s, 1H), 5.70 (t, *J* = 8.2 Hz, 2H), 4.55 (t, *J* = 7.6 Hz, 2H), 2.77 (d, $^{3}J_{PH}$ = 10.6 Hz, 12H, $N(CH_3)_2$), 2.28-2.17 (m, 8H), 1.41-1.27 (m, 72H), 0.90-0.87 (m, 12H) ppm; ^{1}H NMR (400 MHz, [D_8]toluene) 8.83 (s, 1H), 7.88 (d, *J* = 8.2 Hz, 2H), 7.75 (s, 2H), 7.72 (s, 1H), 7.68 (s, 2H), 7.60 (s, 1H), 7.48 (d, *J* = 8.2 Hz, 2H), 7.19 (ddd, *J* = 8.2, 8.2, 1.0 Hz, 2H), 7.05-7.01 (m, 2H), 6.15 (t, *J* = 8.1 Hz, 2H), 4.97 (t, *J* = 7.4 Hz, 2H), 2.52 (d, $^{3}J_{PH}$ = 10.2 Hz, 12H, $N(CH_3)_2$), 2.49-2.09 (m, 8H), 1.51-1.30 (m, 72H), 0.96-0.93 (m, 12H) ppm; $^{13}C\{^{1}H\}$ NMR (100 MHz, $CDCl_3$) 153.3 (C^{15}), 153.1 (C^{10}), 153.0 (C^{7}), 152.6 (C^{8}), 149.8 (two peaks are overlapped, C^{17} C^{21}), 149.3 (two peaks are overlapped, $C^{5}C^{6}$), 140.3 (d, $^{4}J_{cp}$ = 9.3 Hz, C^{13}), 137.7 (C^{19}), 136.5 (C^{12}), 135.7 (C^{20}), 134.5 (C^{1}), 129.2 (C^{3}), 128.3 (C^{4}), 123.9 (C^{18}), 122.6 (C^{14}), 121.8 (C^{11}), 119.1 (C^{22}), 117.8 (C^{16}), 117.0 (C^{9}), 35.4 (d, $^{2}J_{CP}$ = 18.8 Hz, two peaks are overlapped, C^{23} C^{24}), 35.8, 34.4, 32.6, 32.3, 31.6, 30.1, 29.8, 28.4, 28.3, 23.1, 14.5, (many peaks are overlapped) ppm; $^{31}P\{^{1}H\}$ NMR (162 MHz, $CDCl_3$) 140.6 ppm; MS (ESI) *m/z*: 1539 [M + Cl]$^-$; IR (neat): 2922, 2851, 1577, 1481, 1412, 1332, 1158, 977, 758 cm^{-1}; HRMS (ESI) calcd for $C_{92}H_{124}N_6O_8P_2Cl$: 1538.8678, Found: 1538.8668; Anal. Calcd for $C_{92}H_{124}N_6O_8P_2$: C, 73.47; H, 8.31; N, 5.59. Found: C, 73.47; H, 8.37; N, 5.66.

Synthesis of 3: (see Scheme 1(c)) To **1** (148 mg, 0.1 mmol) in toluene (4 mL) at 0 ºC was slowly added a cooled-toluene solution of mCPBA (75%, 23 mg, 0.1 mmol) over 3 min. After stirred at 0 ºC for 1.5 h, the reaction was quenched with saturated aqueous $NaHCO_3$ (2 mL), and stirred at ambient temperature for 30 min. The mixture was transferred into a 50 mL separatory funnel, washed with water (10 mL) and brine (10 mL), dried over Na_2SO_4, and concentrated *in vacuum* to give a crude of 143 mg as a white solid material. Purification by short-plugged column chromatography (SiO_2, toluene/EtOAc = 9/1) led to 44 mg of **3** in 30% yield as white solid powder. ^{1}H NMR (400 MHz, $CDCl_3$) 8.43 (s, 1H), 8.13 (d, *J* = 8.3 Hz, 1H), 7.87 (d, *J* = 8.5 Hz, 1H), 7.84-7.82 (m, 1H), 7.79-7.77 (m, 1H), 7.70 (dd, *J* = 8.1, 7.0 Hz, 1H), 7.59 (dd, *J* = 7.6, 7.3 Hz, 1H), 7.49-7.46 (m, 2H), 7.44 (s, 1H), 7.42 (s, 1H), 7.23 (s, 1H), 7,17 (s, 3H), 6.58 (s, 1H), 5.79-5.71 (m, 2H), 4.61 (t, *J* = 7.6 Hz, 1H), 4.49 (t, *J* = 7.6 Hz, 1H), 4.00 (d, $^{3}J_{PH}$ = 11.3 Hz, 3H), 3.88 (d, $^{3}J_{PH}$ = 8.9 Hz, 3H), 2.36-2.24 (m, 8H), 1.41-1.28 (m, 72H), 0.92-0.87 (m, 12H) ppm; ^{1}H NMR (400 MHz, [D_8]toluene) 8.82 (s, 1H), 7.98 (d, *J* = 8.2 Hz, 1H), 7.95 (s, 1H), 7.77 (s, 1H), 7.69-7.59 (m, 5H), 7.49 (s, 1H), 7.48 (d, *J* = 8.2 Hz, 1H), 7.26 (m, 2H), 7.16-6.93 (m, 2H), 7.61 (s, 1H), 6.20 (t, *J* = 8.0 Hz, 1H), 6.11 (t, *J* = 8.0 Hz, 1H), 4.90 (t, *J* = 7.6 Hz, 1H), 4.77 (t, *J* = 7.6 Hz, 1H), 3.55 (d, $^{3}J_{PH}$ = 11.3 Hz, 3H), 3.45 (d, $^{3}J_{PH}$ = 8.9 Hz, 3H), 2.47-2.29 (m, 8H), 1.33-1.28 (m, 72H), 0.96-0.92 (m, 12H) ppm; $^{13}C\{^{1}H\}$ NMR (100 MHz, $CDCl_3$) 153.5 (C^{40}), 153.3 (C^{7}), 153.0 (C^{8}), 152.8 (C^{15}), 152.7 (C^{16}), 147.6 (C^{26}), 147.2 (d, $J_{C,P}$ = 3.8 Hz, C^{30}), 146.34 (C^{24}), 146.28 (C^{19}), 146.1 (d, $J_{C,P}$ = 6.91 Hz, C^{17}), 140.41 (C^{13}), 140.38 (C^{6}), 140.31 (C^{14}), 140.27 (C^{5}), 138.0 (C^{38}), 137.2 (C^{27}), 136.9 (d, $J_{C,P}$ = 1.9 Hz, C^{32}), 136.6 (C^{23}), 135.8 (C^{21}), 135.3 (C^{29}), 134.4 (d, $J_{C,P}$ = 4.5 Hz, C^{23}), 133.0 (C^{28}), 132.9 (C^{36}), 129.7 (C^{2}), 129.6 (C^{11}), 129.4 (C^{3}), 129.2 (C^{10}), 128.7 (C^{34}), 128.4 (C^{22}), 128.24 (C^{33}), 128.20 (C^{20}), 123.6 (C^{12}), 123.0 (C^{1}), 122.5 (C^{9}), 122.3 (C^{9}), 119.3 (C^{37}), 118.8 (C^{25}), 117.03 (C^{39}), 116.99 (C^{31}), 116.93 (C^{18}), 56.0 (d, $J_{C,P}$ = 6.2 Hz, C^{42}), 50.2 (C^{41}), 36.0, 35.9, 34.5, 34.4, 33.1, 32.3, 32.1, 31.5, 31.4, 30.1 (many peaks are overlapped), 29.8 (many peaks are overlapped), 28.4, 28.3, 23.1 (many peaks are overlapped), 14.5 (many peaks are overlapped) ppm; $^{31}P\{^{1}H\}$ NMR (162 MHz, $CDCl_3$) 125.7, -13.6 ppm; MS (ESI) *m/z*: 1528 [M + Cl]$^-$; IR (neat): 2922, 2851, 1578, 1482, 1412, 1352, 1146, 1029, 760 cm^{-1}; HRMS (ESI) calcd for $C_{90}H_{118}N_4O_{11}P_2Cl$: 1527.7966 [M + Cl]$^-$, Found : 1527.7967.

Synthesis of 1•(AuCl)$_2$ and 3•AuCl: (see Scheme 2)

For **1**•2AuCl: Under N_2 atmosphere, a solution of **1** (148 mg, 0.1 mmol) in toluene (2 mL) underwent addition of $AuCl•S(CH_3)_2$ (71 mg, 0.24 mmol), and the mixture was stirred for 40 min, consumption of **1** was monitoring by TLC. After all the volatiles had been evaporated, 174 mg of as white powder materials, corresponding to **1**•$(AuCl)_2$ complex was isolated in quantitative yield. ^{1}H NMR (400 MHz, $CDCl_3$) 8.33 (s, 1H), 7.92-7.90 (m, 4H), 7.64-7.58 (m, 4H), 7.46 (s, 2H), 7.31 (s, 1H), 7.29 (s, 2H), 7.24 (s, 1H), 6.82 (s, 1H), 5.77 (t, *J* = 8.0 Hz, 2H), 4.44 (t, *J* = 7.3 Hz, 2H), 4.02 (d, $^{3}J_{P,H}$ = 13.8 Hz, 6H), 2.30-2.17 (m, 8H), 1.45-1.27 (m, 72H), 0.90-0.87 (m, 12H) ppm; $^{13}C\{^{1}H\}$ NMR (100 MHz, $CDCl_3$) 53.2 (d, $J_{C,P}$ = 1.7 Hz, C^{7}), 153.1 (two peaks are overlapped, C^{17} C^{21}), 152.2 (C^{15}), 152.0 (C^{10}), 145.3 (C^{6}), 144.6 (C^{5}), 140.2 (C^{13}), 140.1 (two peaks are overlapped, $C^{12}C^{19}$), 137.9 (d, $J_{C,P}$ = 1.9 Hz, C^{8}), 137.0 (C^{1}), 136.0 (C^{4}), 135.7 (C^{2}), 130.2 (C^{20}), 130.0 (C^{18}), 129.6 (C^{3}), 127.5 (C^{14}), 123.4 (C^{11}), 123.2 (C^{9}), 119.0 (C^{16}), 118.3 (C^{22}), 55.1 ($POCH_3$, C^{23}), 36.0, 34.4, 32.2 (many peaks are overlapped), 31.2, 30.0 (many peaks are overlapped), 29.9 (many peaks are overlapped), 29.9, (many peaks are overlapped), 29.8, 29.7 (many peaks are overlapped), 28.2, 28.1, 23.0, 22.9, 14.4 ppm; $^{31}P\{^{1}H\}$ NMR (162 MHz, $CDCl_3$) 99.4 ppm; MS (ESI) *m/z*: 1906 [M—Cl]$^+$; IR (neat): 2925, 2857, 1483, 1408, 1328, 1148, 1029, 905, 759, 599 cm^{-1}; HRMS (ESI) calcd for $C_{90}H_{118}Au_2ClN_4O_{10}P_2$: 1905.7343 [M - Cl]$^+$, Found: 1905.7394.

For **3**•AuCl Under N_2 atmosphere, a solution of **3** (111 mg, 0.074 mmol) in toluene (1.2 mL) underwent addition of $AuCl•S(CH_3)_2$ (26 mg, 0.089 mmol), and the reaction mixture was stirred for 30 min, consumption of **3** was monitoring by TLC. After all the volatiles had been evaporated, the crude products were purified by short-plugged silica-gel column chromatography (eluent: hexane/EtOAc, 1/1) to afford 56 mg of **3**•AuCl as white powder materials in 63% yield. ^{1}H NMR (400 MHz, $CDCl_3$) 8.40 (s, 1H), 8.11 (d, *J* = 8.4 Hz, 1H), 7.95 (d, *J* = 8.4 Hz, 1H), 7.88 (d, *J* = 8.4 Hz, 1H), 7.78 (d, *J* = 8.4 Hz, 1H), 7.72 (dd, *J* = 8.4, 8.4 Hz, 1H), 7.63 (dd, *J* = 8.4, 8.4 Hz, 1H), 7.56 (s, 1H), 7.53-7.46 (m, 2H), 7.39 (s, 1H), 7.21 (s, 1H), 7.20 (s, 1H), 7.19 (s, 1H), 7.15 (s, 1H), 6.73 (s, 1H), 5.81 (t, *J* = 8.0 Hz, 1H), 5.77 (t, *J* = 8.3 Hz, 1H), 4.51 (t, *J* = 8.1 Hz, 1H), 4.50 (t, *J* = 8.2 Hz, 1H), 4.07 (d, $^{3}J_{P,H}$ = 13.9 Hz, 3H), 3.99 (d, $^{3}J_{P,H}$ = 11.4 Hz, 3H), 2.36-2.21 (m, 8H), 1.48-1.27 (m, 72H), 0.90-0.87 (m, 12H) ppm; $^{13}C\{^{1}H\}$ NMR (100 MHz, $CDCl_3$) 153.6 (two peaks are overlapped, C^{19} C^{38}), 153.1 (C^{6}), 152.8 (two peaks are overlapped, C^{32} C^{40}), 152.7 (C^{5}), 152.5 (C^{13}), 152.0 (C^{14}), 146.8 (d, $J_{C,P}$ = 6.4 Hz, C^{17}), 146.3 (d, $J_{C,P}$ = 6.4 Hz, C^{30}), 144.3 (d, $J_{C,P}$ = 5.5 Hz, C^{24}), 143.8 (d, $J_{C,P}$ = 4.8 Hz, C^{26}), 140.44 (C^{20}), 140.36 (C^{37}), 140.3 (C^{35}), 140.2 (C^{33}), 138.0 (d, $J_{C,P}$ = 1.7 Hz, C^{16}), 137.1 (d, $J_{C,P}$ = 4.8 Hz, C^{7}),

136.1 (C^{23}), 135.9 (C^{22}), 135.8 (C^{29}), 135.5 (C^{15}), 135.4 (C^{18}), 133.6 (d, $J_{C,P}$ = 3.6 Hz, C^{31}), 130.0 (C^{36}), 129.9 (C^{21}), 129.8 (C^{34}), 129.7 (C^{28}), 129.3 (C^{27}), 128.8 (C^{3}), 128.1 (C^{10}), 127.8 (C^{11}), 123.7 (C^{2}), 123.0 (C^{9}), 122.8 (C^{4}), 122.5 (C^{12}), 119.2 (C^{1}), 118.4 (d, $J_{C,P}$ = 3.8 Hz, C^{18}), 117.0 (d, $J_{C,P}$ = 4.3 Hz, C^{39}), 116.5 (C^{25}), 56.0 (d, $^{2}J_{C,P}$ = 6.0 Hz, C^{42}), 54.7 (d, $^{2}J_{C,P}$ = 2.9 Hz, C^{41}), 36.0, 34.4, 33.2, 32.3 (many peaks are overlapped), 31.8, 30.4, 30.1 (many peaks are overlapped), 30.0 (many peaks are overlapped), 29.8, 29.7, 23.0 (many peaks are overlapped), 14.5 (many peaks are overlapped) ppm; $^{31}P\{^{1}H\}$ NMR (162 MHz, $CDCl_3$) 112.8, -7.60 ppm; MS (ESI) *m/z*: 1760 $[M + Cl]^-$; IR (neat): 2921, 2849, 1483, 1408, 1328, 1145, 1041, 914, 759 cm^{-1}; HRMS (ESI) calcd for $C_{90}H_{118}AuCl_2N_4O_{11}P_2$: 1759.7320 $[M + Cl]^-$, Found: 1759.7350.

Representative procedure for Au-catalyzed dimerization of terminal alkynes: (see Scheme 3) Under N_2 atmosphere, the bis-Au catalyst (0.01 mmol) in a 25 mL two-necked flask was dissolved in toluene (5 mL; containing traces of water), and the starting alkynes of ethynylbenzene (102 mg, 1 mmol) and the other partner 1-octyne (165 mg, 1.5 mmol) were added. After addition of AgOTf (5.0 mg, 0.02 mmol) at room temperature, the reaction was conducted for 20 h. The solvent was evaporated off, and filtered through a short-plugged column chromatography to give a crude product. The crude materials consisted of just starting alkynes and/or product **7a**, **7b**, and **7c** because of clean reaction progress: thus, chemical yields and molar ratios of products were determined in the crude state. All dimeric adducts were identical to the authentic samples that we previously reported.[7b,9]

Representative procedure for Au-catalyzed hydration of internal alkynes: (see Scheme 4) Complex **1**•$(AuCl)_2$ (17 mg, 0.01 mmol) was added under Ar to a solution of 3-octyne (0.07 mL, 0.5 mmol) in toluene-d_8 (1 mL) and H_2O (0.05 mL, 2.5 mmol). The mixture was stirred at room temperature for 5 min, AgOTf (3 mg, 0.012 mmol) was then added, and the whole system was immersed in a 50 ºC preheated oil bath. After stirred for 1 h, the reaction mixture was allowed to cool to ambient temperature. Purification by short-plug silica-gel column chromatography with use of a Pasteur pipette and $[D_8]$toluene as eluent gave a colorless C_7D_8 solution. ^{1}H NMR spectroscopy determined the chemical yields and product distribution (proportions of **7f** and **7g**).[9] ^{1}H NMR spectroscopic data for **7f** and **7g** were identical to those for commercially available authentic sample.

Representative procedure for Rh-catalyzed hydroformylation of styrene: (see Scheme 5) The hydroformylation reactions were carried out in a glass-lined, 50 mL stainless steel autoclave containing a magnetic stirring bar, then the autoclave was closed and flushed twice with vacuum/N_2. To the vessel were added toluene (8 mL), styrene (10 mmol), *n*-decane (0.5 mL), 1 mL toluene solution of $Rh(acac)(CO)_2$ (2 µmol), and 1 mL toluene solution of appropriate ligand. After pressurized at 20 bar (CO/H_2 1:1) and heated at appropriate temperature for the adequate time, the autoclave was allowed to cool to ambient temperature before being depressurized. The reaction mixture was analyzed by GC using a WCOT fused-silica gel column chromatography (25 m x 0.25 mm) and by ^{1}H NMR.

Supporting Information (see footnote on the first page of this article): The ^{1}H and $^{13}C\{^{1}H\}$ NMR spectra of all new compounds.

Acknowledgments

JSPS Grant-in-Aid for Scientific Research (C), Grant Number 19K05426, which supported TI in this work, is gratefully thanked for generous funding. The authors thank Dr. Toshiyuki Iwai and Dr. Takatoshi Ito at ORIST for gentle assistance with HRMS. Prof. Dr. Schramm, M. P. at CSULB are gratefully thanked for helpful discussions. SH gratefully acknowledges the University of Carthage and the Tunisian Ministère de l'Enseignement Supérieur et de la Recherche Scientifique for the financial support.

[1] a) R. Breslow, *Acc. Chem. Res.* **1995**, *28*,146-153; b) R. J. Hooley, J. Rebek, Jr. *Chemistry & Biology* **2009**, *16*, 255-264, and references therein; c) P. D. Frischmann, M. J. MacLachlan, *Chem. Soc. Rev.* **2013**, *42*, 871-890, and references therein.

[2] a) D. Ringe, G. A. Petsko, *Science* **2008**, *320*, 1428-1429; b) X. Y. Zhang, K. N. Houk, *Acc. Chem. Res.* **2005**, *38*, 379-385.

[3] a) J. R. Moran, S, Karbach, D. J. Cram, *J. Am. Chem. Soc.* **1982**, *104*, 5826-5828; b) A. R. Renslo, J. Rebek, Jr., *Angew. Chem. Int. Ed.* **2000**, *39*, 3281-3283; c) T. Chavagnan, D. Sémeril, D. Matt, L. Toupet, *Eur. J. Org. Chem.* **2017**, 313-323.

[4] a) Mini-reviews, A. C. H. Jans, X. Caumes, J. N. H. Reek, *ChemCatChem.* **2019**, *11*, 287-297; b) Digest review, T. Iwasawa, *Tetrahedron Lett.*, **2017**, *58*, 4217-4228; c) N. Natarajan, E. Brenner, D. Sémeril, D. Matt, J. Harrowfield, Eur. J. Org. Chem., 2017, 6100-6113.

[5] F. Diederich, *Angew. Chem. Int. Ed.* **2007**, *46*, 68-69.

[6] F. Wöhler, *Ann. Chim. Phys.* **1828**, *37*, 330.

[7] a) T. Iwasawa, Y. Nishimoto, K. Hama, T. Kamei, M. Nishiuchi, Y. Kawamura, *Tetrahedron Lett.* **2008**, *49*, 4758-4762; b) M. Kanaura, N. Endo, M. P. Schramm, T. Iwasawa, *Eur. J. Org. Chem.* **2016**, 4970-4975.

[8] N. Endo, M. Kanaura, M. P. Schramm, T. Iwasawa, *Eur. J. Org. Chem.* **2016**, 2514-2521.

[9] N. Endo, M. Inoue, T. Iwasawa, *Eur. J. Org. Chem.* **2018**, 1136-1140.

[10] P. P. Castro, G. Zhao, G. A. Masangkay, C. Hernandez, L. M. Gutierrez-Tunstad, *Org. Lett.* **2004**, *6*, 333-336.

[11] No resonances of the "in-in" isomer was observed in the ^{1}H NMR spectrum of the crude reaction mixture.

[12] The oxidation with mCPBA led to 24% of di-phosphate derivative and 46% of unreacted *iso*-**1** was recovered.

[13] In compound **5**, crystallographic analysis revealed that for steric reason, the two $PN(CH_3)_2$ moieties point outside from the cavity, see ref 9.

[14] V. A. Azov, B. Jaun, F. Diederich, *Helv. Chim. Acta.* **2004**, *87*, 449-462.

[15] M. Inoue, K. Ugawa, T. Maruyama, T. Iwasawa, *Eur. J. Org. Chem.* **2018**, 5304-5311.

[16] M. P. Schramm, M. Kanaura, K. Ito, M. Ide, T. Iwasawa, *Eur. J. Org. Chem.* **2016**, 813-820.

[17] a) R. Bellini, S. H. Chikkali, G. Berthon-Gelloz, J. N. H. Reek, *Angew. Chem., Int. Ed*. **2011**, 50, 7342-7345; b) V. Bocokic, A. Kalkan, M. Lutz, A. L. Spek, D. T. Gryko, J. N. H. Reek, *Nat. Commun* **2013**, *4*, No. 2670; c) M. Jouffroy, R. Gramage-Doria, D. Armspach, D. Sémeril, W. Oberhauser, D. Matt, L. Toupet, *Angew. Chem. Int. Ed*. **2014**, *53*, 3937-3940.

[18] a) D. Sémeril, C. Jeunesse, D. Matt, L. Toupet, *Angew. Chem. Int. Ed*. **2006**, *45*, 5810-5814; b) D. Sémeril, D. Matt, L. Toupet, *Chem. Eur. J.* **2008**, *14*, 7144-7155; c) D. Sémeril, D. Matt, L. Toupet, W. Oberhauser, C. Bianchini, *Chem. Eur. J*. **2010**, *16*, 13843-13849.

[19] a) M. E. Broussard, B. Juna, S. G. Train, W.-J. Peng, S. A. Laneman, G. G. Stanley, *Science* **1993**, *260*, 1784-1788; b) D. A. Aubry, N. N. Bridges, K. Ezell, G. G. Stanley, *J. Am. Chem. Soc.* **2003**, *125*, 11180-11181; c) D. G. H. Hetterscheid, S. H. Chikkali, B. de Bruin, J. N. H. Reek, *ChemCatChem* **2013**, *5*, 2785-2793.

Received: ((will be filled in by the editorial staff))
Published online: ((will be filled in by the editorial staff))

QUESTIONS-SUGGESTIONS

Are you sure of the circle labeling of 2 and 5 (e and f in figure 2) (orientation of PNMe2 is out from the cavity)?

Can you change **1**•2AuCl with **1**•$(AuCl)_2$ and **4**•2AuCl with **4**•$(AuCl)_2$ in Schemes 2, 3 and 4.

In Scheme 4, part b: you have to change **3**•2AuCl with **3**•AuCl and **6**•2AuCl with **6**•AuCl

In Scheme 3, for clarity raison, please remove columns ethylbenzene and 1-octyne in table (a) and in table (b) remove column 1-octyne. Can you add under toluene "water (traces)"

In Scheme 4, for clarity raison, please remove column 1-phenyl-1butyne in table (a) and in table (b) remove column 3-octyne

In Supplementary Materials, please add $\{^1H\}$ after ^{13}C to write "$^{13}C\{^1H\}$ NMR" pages 3, 6, 9, 12, 14and 16. Pages 13 and 14, can you change **1**•2AuCl with of **1**•$(AuCl)_2$**.**

Entry for the Table of Contents

Layout 2:

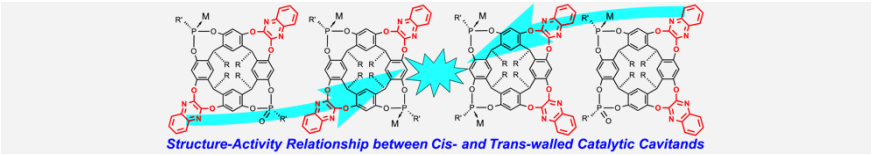

Three new cis-diquinoxaline spanned cavitands were synthetized. These cis-diphosphinated derivatives were assigned in homogeneous catalysis. Results were ranked with those obtained with their trans-diphosphinated analogues. The Structure-activity relationship realized with these cis- or trans-flanked cavitands shows that the cis- or trans-positioning of the catalytic center has a direct effect either on activity or on regioselectivity of a catalytic reaction.

Mami Inoue, Shinsuke Kamiguchi, Katto Ugawa, Shaima Hkiri, Jules Bouffard, David Sémeril,* and Tetsuo Iwasawa* Page No. – Page No.

Evaluation of Catalytic Capability of cis- and trans-Diquinoxaline Spanned Cavitands

Keywords: Introverted ligand / Cis-spanned cavitands / Diquinoxaline-extended resorcin[4]arene / Gold and Rhodium catalysis

Supporting Information

^{1}H NMR and ^{13}C NMR spectra for all new compounds of *cis*-**1**, *cis*-**2**, *cis*-**3**, **1**•$(AuCl)_2$ and **3**•AuCl.